Supplementary Material:

Laser-chirp controlled terahertz wave generation from air-plasma

Xing Xu,[1,2,3,4] Yindong Huang,[2] Zhelin Zhang,[5,6,7] Jinlei Liu,[8] Jing Lou,[2] Mingxin Gao,[2] Shiyou Wu,[1,3,4] Guangyou Fang,[1,3,4] Zengxiu Zhao,[8] Yanping Chen,[6,7] Zhengming Sheng,[5,6,7] and Chao Chang[2,1]

[1)]*Aerospace Information Research Institute, Chinese Academy of Sciences, Beijing 100094, China*

[2)]*Innovation Laboratory of Terahertz Biophysics, National Innovation Institute of Defense Technology, Beijing 100071, China*

[3)]*Key Laboratory of Electromagnetic Radiation and Sensing Technology, Chinese Academy of Sciences, Beijing 100190, China*

[4)]*School of Electronic, Electrical and Communication Engineering, University of Chinese Academy of Sciences, Beijing 100049, China*

[5)]*Tsung-Dao Lee Institute, Shanghai Jiao Tong University, Shanghai 200240, China*

[6)]*Key Laboratory for Laser Plasmas, School of Physics and Astronomy, Shanghai Jiao Tong University, Shanghai 200240, China*

[7)]*Collaborative Innovation Center of IFSA, Shanghai Jiao Tong University, Shanghai 200240, China*

[8)]*Department of Physics, National University of Defense Technology, Changsha 410073, China*

(*Electronic mail: gwyzlzssb@pku.edu.cn)

(*Electronic mail: yanping.chen@sjtu.edu.cn)

(*Electronic mail: yindonghuang@nudt.edu.cn)

I. LINEAR DIPOLE ARRAY (LDA) MODEL

The linear dipole model used in the simulation of the terahertz (THz) wave generation has been reported previously[1,2]. In this section, we will give a brief introduction of this model. The core idea of the linear dipole array (LDA) model is to treat the THz emissions as the coherent superposition of the THz wave from an array of point sources.

The combined electric field parallel to the polarization of the incident fundamental wave (FW) can be written as

$$E_{\mathrm{com}}(t) = E_{\omega}(t) + E_{2\omega}(t), \tag{Eq. S1}$$

where ω is the frequency of the FW, E_{ω} and $E_{2\omega}$ are the amplitude of the FW and its second harmonic (SH). For each point source of the linear arrays in the filament, it can be considered as the localized dipole formed by the spatial separation between the ionized electrons and the left ions, as shown in FIG. S1.

Each localized dipole $dP(z,t',t;\omega_{THz})$ can be written as

$$dP(z,t,t';\omega_{\mathrm{THz}}) = r_m dq(z,t')\exp(-j\omega_{\mathrm{THz}}t), \tag{Eq. S2}$$

where r_m is the spatial separation between positive and negative charge center, $dq(z,t')$ is the localized charge at z, j is the imaginary unit and ω_{THz} is the corresponding THz frequency. As is mentioned in Ref.[3], the estimated average velocity is of the order of $\sim 10^6$ m/s, and the plasma frequency ω_p is about 1 THz, which can be applied to deduce that $r_m \sim 1$ μm. The corresponding emission of THz wave from each localized dipole can be expressed as

$$dE^{\mathrm{THz}}_{\mathrm{dipole}}(z,t,t';\omega_{\mathrm{THz}}) \propto \frac{\partial^2}{\partial t^2}[dP(z,t,t';\omega_{\mathrm{THz}})]\exp[j\Phi(z)]. \tag{Eq. S3}$$

Here, we consider the one dimensional (1D) generation and propagation of the THz waves from each localized dipole. The coherent superposition of THz waves from the whole filament can

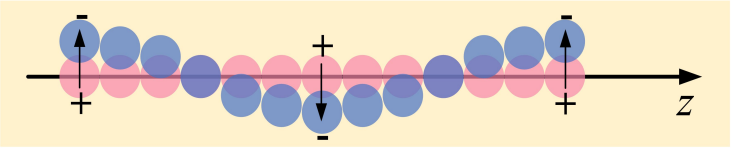

FIG. S1. Sketch of the localized dipole array along the filament. The blue and red spheres indicate the spatial separation of the ionized electrons and the left ions.

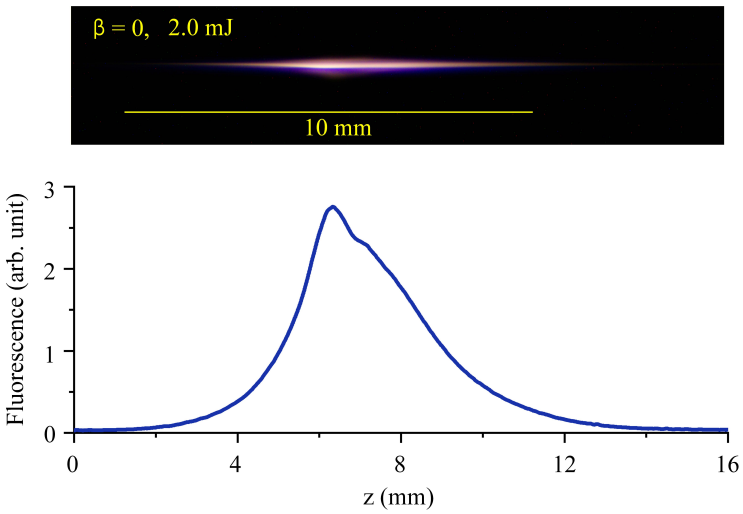

FIG. S2. One typical filament fluorescence and the corresponding integrated intensity

therefore be written as

$$E_{\mathrm{THz}}(\omega_{\mathrm{THz}},t) = \int_0^{\tau}\int_{filament} dE^{\mathrm{THz}}_{\mathrm{dipole}}(z,t,t';\omega_{\mathrm{THz}}), \qquad \text{(Eq. S4)}$$

where the integration ranges cover the whole pulse duration and the filament length.

II. LASER ENERGY- AND CHIRP- DEPENDENT PLASMA FLUORESCENCE

By using a commercial charge-coupled device (CCD) camera arranged on a stereomicroscope, the plasma fluorescence can be traced from the CCD image. Each CCD image is acquired from 2 s exposure time, which corresponds to about 2000 shoots of laser pulses.

We use the chirp parameter β to value the degree of chirp, which can be expressed as[4]

$$\beta \triangleq \sqrt{(\tau_p/\tau_0)^2 - 1}, \qquad \text{(Eq. S5)}$$

where τ_p is the pulse duration of the chirped pulse, and $\tau_0 = 99$ fs is the Fourier-limited pulse duration ($\beta = 0$). The plasma fluorescence obtained by the CCD exhibits a shining line of filament, as shown in FIG. S2. To be applicable to our 1D-LDA model, the fluorescence images are integrated along the vertical direction of the z axis. In the bottom of FIG. S2, we show one typical result of the integrated fluorescence when $\beta = 0$ and the input laser energy $= 2$ mJ.

FIG. S3 show the laser energy- and chirp-dependent plasma fluorescence. The intensity of each horizontal line in FIG. S3 corresponds to the plasma fluorescence along the z axis. Since the

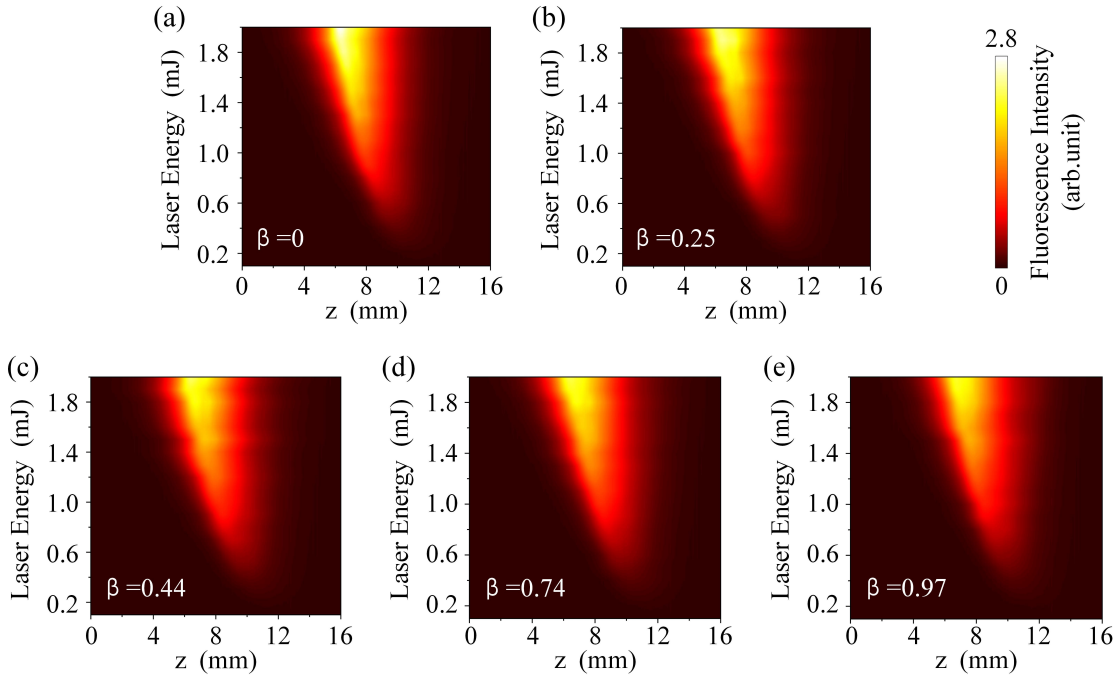

FIG. S3. Fluorescence of the filament along z axis at different laser energies under the pulse duration of (a) 99 fs, (b) 102 fs, (c) 108 fs, (d) 123 fs and (e) 138 fs.

fluorescence intensity of the filaments is positively correlated with the plasma density, the obtained line fluorescence intensity can be used to estimate the spatial distribution of the plasma density. Actually, during the process of filamentation, laser pulse will exhibit non-linear effects such as the Kerr effect and self-focusing effect, which usually requires large computational resources to calculate the temporal and spatial evolution of the focusing pulse[5]. The fluorescence intensity of the filament captured by the CCD camera can offer the realistic picture of the density distribution of the spatial plasma.

To compare the detailed intensities on the plasma fluorescence, we provide the spatial distributions of the fluorescence under different laser chirps for three typical laser energies, as shown in FIG. S4(a)-(c). It can be found that the peaks and general spatial shapes of fluorescence are quite similar for different chirps, implying the similar plasma properties. Therefore, we can avoid the complex calculations for various nonlinear processes on the field strength (*e.g.*, by using the unidirectional pulse propagation equation (UPPE)[6] or other complicated method to calculate the evolution of the electric field), and instead use the real plasma properties for simulation.

As is described in FIG. 2 of the main text, the THz wave generation will exhibit a yield minimum under the suitable laser chirp and laser energy. In FIG. S4(d), the plasma fluorescence for

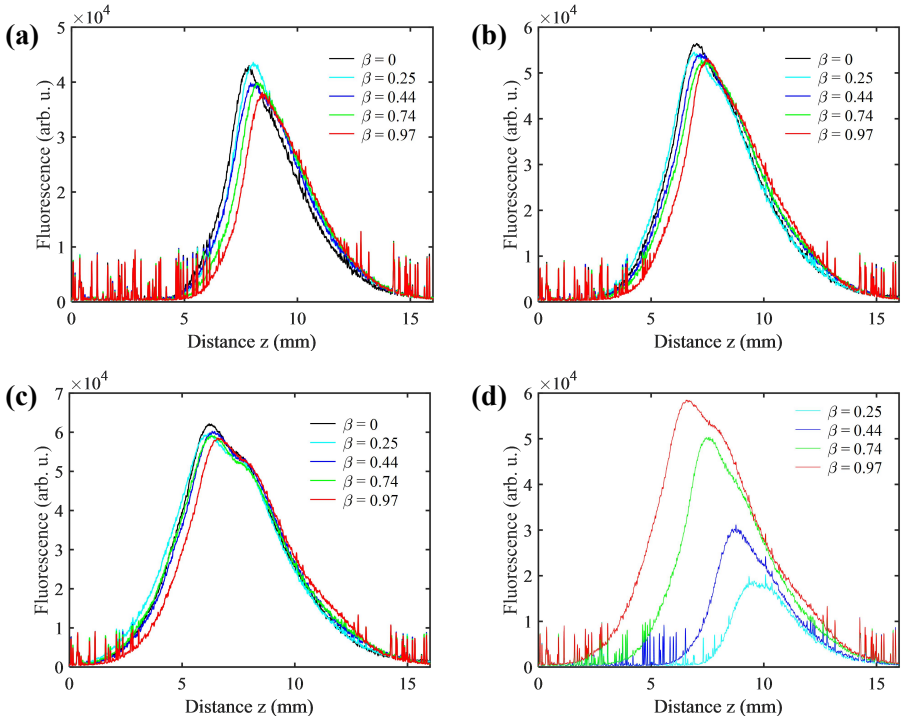

FIG. S4. The detailed intensities of the plasma fluorescence along the z axis at different laser chirps are compared when the laser input is 1 mJ (a), 1.5 mJ (b) and 2 mJ (c). (d) show the plasma properties for the THz generation minima under different laser chirps.

the THz yield minima are compared to demonstrate the difference between the plasma length and shapes. This result gives a strong clue that the laser-chirp controlled THz wave generation not only dependents on the plasma length[7], but also should include the relative phase difference between the two colors. Each fluorescence curve under a fixed laser energy contains 3072 data points. In order to filter out the noise, a moving average filter is adopted to smooth the data with the span for the moving average of 20. As an example, the comparison of fluorescence intensity distribution before and after filtering under the laser energy of 0.5 mJ is show in FIG. S5.

III. PHASE MATCHING BETWEEN TERAHERTZ WAVE AND LASER

In this section, we will discuss the phase matching between the THz wave and laser pulse. When the THz wave propagate through a laser-prepared filament, the screening of the charging carriers (mainly electrons) will introduce a broadband resonant absorption of the THz wave[8]. This screening effect can modify the relative dielectric constant from a Drude line to a Lorentz type,

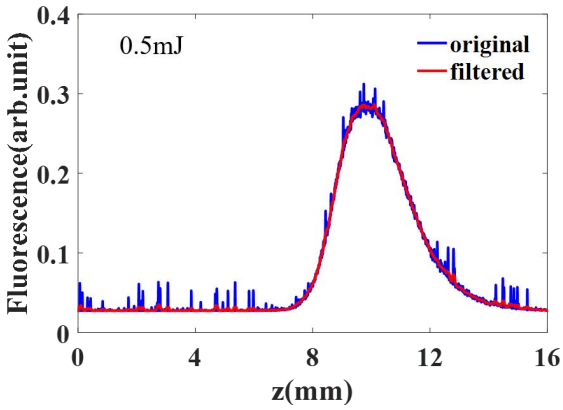

FIG. S5. The comparison of fluorescence intensity distribution before and after filtering under the laser energy of 0.5 mJ. The blue curve is the original data and the red curve is the filtered data using the moving average filter with the span of 20.

which can be written as

$$\varepsilon(\Omega) = 1 - \frac{\omega_p^2}{\Omega^2 - \omega_p^2/2 + i\Gamma\Omega}, \tag{Eq. S6}$$

where Ω is the THz frequency, $\omega_p = \sqrt{(N_e e^2)/(\varepsilon_0 m_e)}$ is the plasma frequency, and Γ is the collision frequency.

Then, the complex refractive index of the filament is defined as

$$\widetilde{n_\Omega} = \sqrt{\varepsilon(\Omega)} = n_\Omega + i\kappa_\Omega, \tag{Eq. S7}$$

where the real part n_Ω is the refractive index and the imaginary part κ_Ω is the extinction coefficient of the plasma media.

The refractive indexes difference $\Delta n'$ between the THz wave and laser can be written as

$$\Delta n' = n_{\omega_0} - n_\Omega \simeq 1 - \left(\sqrt{1 - \frac{\omega_p^2}{\Omega^2 - \omega_p^2/2 + i\Gamma\Omega}}\right)_{Re}, \tag{Eq. S8}$$

where ω_0 indicates the 800 nm pulse, Ω is the THz frequency, ω_p is the plasma frequency and Γ is the collision frequency. The coherent buildup length L_c can be expressed as

$$L_c(\Omega) = \frac{2\pi c}{\Delta n' \Omega}. \tag{Eq. S9}$$

As shown in FIG. S6, we show the calculated collision-frequency-dependent coherent buildup length for three different THz frequencies by using Eq. S9. The plasma frequency ω_p is set to be 1 THz. Obviously, L_c grows with increasing collision frequency, suggesting the importance of

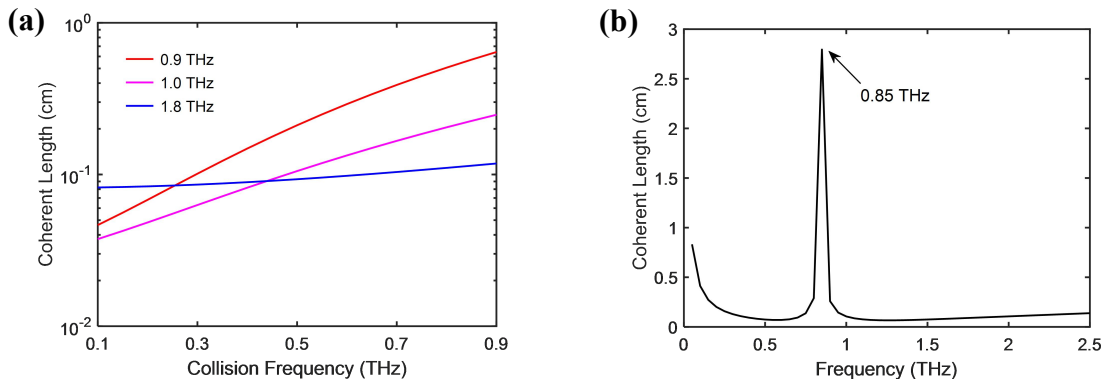

FIG. S6. (a) The collision frequency Γ dependent coherent length L_c for 0.9 THz (red line), 1.0 THz (purple line), and 1.8 THz (blue). (b) One calculated coherent length L_c for different THz frequencies.

plasma relaxation in phase matching of THz waves. It is worth noting that the growth speed at 0.9 THz is much faster than that at 1.0 THz and 1.8 THz.

We have also calculated the coherence lengths for different frequencies of THz wave under one collision frequency of 0.5 THz, as shown in FIG. S6(b). It can be found that the coherence length of the THz wave peaks at 0.85 THz, corresponding to a coherence length of about 2.75 cm. This length is larger than the typical length of the filament produced by the commercially available femtosecond laser under the major experimental conditions. Meanwhile, for the other THz frequency point that is away from the peak frequency, the coherence length will decrease very rapidly, resulting in a coherent suppression of THz radiations at these frequency points. This phenomenon introduces the asynchronous variation of the generating spectrum, which can be found in FIG. 6 of the main text.

REFERENCES

[1]Z. Zhang, Y. Chen, M. Chen, Z. Zhang, J. Yu, Z. Sheng, and J. Zhang, "Controllable terahertz radiation from a linear-dipole-array formed by a two-color laser filament in air," Phys. Rev. Lett. **117**, 243901 (2016).

[2]Z. Zhang, Y. Chen, S. Cui, F. He, M. Chen, Z. Zhang, J. Yu, L. Chen, Z. Sheng, and J. Zhang, "Manipulation of polarisations for broadband terahertz waves emitted from laser plasma filaments," Nat. Photonics **12**, 554–559 (2018).

[3]Y. Huang, Z. Xiang, X. Xu, *et al.*, "Localized-plasma-assisted rotational transitions in the terahertz region," Phys. Rev. A **103**, 033109 (2021).

[4]U. Saalmann, S. K. Giri, and J. M. Rost, "Adiabatic passage to the continuum: Controlling ionization with chirped laser pulses," Phys. Rev. Lett. **121**, 153203 (2018).

[5]Z. Zhang, N. Panov, V. Andreeva, Z. Zhang, A. Slepkov, D. Shipilo, M. D. Thomson, T.-J. Wang, I. Babushkin, A. Demircan, U. Morgner, Y. Chen, O. Kosareva, and A. Savel'ev, "Optimum chirp for efficient terahertz generation from two-color femtosecond pulses in air," Appl. Phys. Lett. **113**, 241103 (2018).

[6]M. Kolesik and J. V. Moloney, "Nonlinear optical pulse propagation simulation: From maxwell's to unidirectional equations," Phys. Rev. E **70**, 036604 (2004).

[7]Y. S. You, T. I. Oh, and K. Y. Kim, "Off-axis phase-matched terahertz emission from two-color laser-induced plasma filaments," Phys. Rev. Lett. **109**, 183902 (2012).

[8]Z. Zheng, Y. Huang, Q. Guo, *et al.*, "Filament characterization via resonance absorption of terahertz wave," Phys. Plasmas **24**, 103303 (2017).